Journal Name

RSCPublishing

COMMUNICATION

Polar Stacking of Molecules in Liquid Chloroform

Cite this: DOI: 10.1039/xoxxoooooox

J. J. Shephard,[a,b] A. K. Soper,[c] S. K. Callear,[c] S. Imberti,[c] J. S. O. Evans[b] and C. G. Salzmann[a]*

Received ooth January 2012,
Accepted ooth January 2012

DOI: 10.1039/xoxxoooooox

www.rsc.org/

Using neutron diffraction and the isotopic substitution technique we have investigated the local structure of liquid chloroform. A strong tendency for polar stacking of molecules with collinear alignment of dipole moments is found. We speculate that these polar stacks contribute to the performance of chloroform as a solvent. (50 words)

The dissolution of chemical species in solvents is of fundamental importance for the purification of chemical compounds and for solution chemistry in general. The capability of a solvent to dissolve chemical species is often attributed to its 'polarity' and bulk macroscopic properties such as the relative permittivity or the refractive index are often discussed in this context. However, these approaches only lead to a rather qualitative understanding of the properties of solvents.[1, 2] In fact, there is a growing realization that only knowledge of the exact microscopic properties of solvents – the local molecular interactions and structure – will lead to a complete and quantitative understanding of their properties.[1-3]

Chloroform ($CHCl_3$) is capable of dissolving many substances at high concentrations, and it is used extensively in the chemistry lab as well as in the chemical and pharmaceutical industries. Solutes include vitamins, alkaloids, antibiotics, polymers, dyes and pesticides.[4] Furthermore, a wide range of natural products are extracted from plant materials using $CHCl_3$.[5, 6] Due to its excellent solvent properties $CHCl_3$ is the most frequently used solvent for solution NMR measurements.[7]

Here we investigate the local structure of liquid $CHCl_3$ in detail using neutron diffraction and we discuss possible links between local structure and the performance of $CHCl_3$ as a solvent. Figure 1 shows the experimental neutron diffraction data which were fitted using the empirical potential structure refinement (*EPSR*) technique.[8, 9] The differences between the three experimental diffraction datasets in Figure 1 are caused by the different neutron scattering properties of ^{1}H and D, and this information is used by *EPSR* to produce a representative 3D structural model consistent with the experimental diffraction data (further details are provided in the *ESI*).[10, 11]

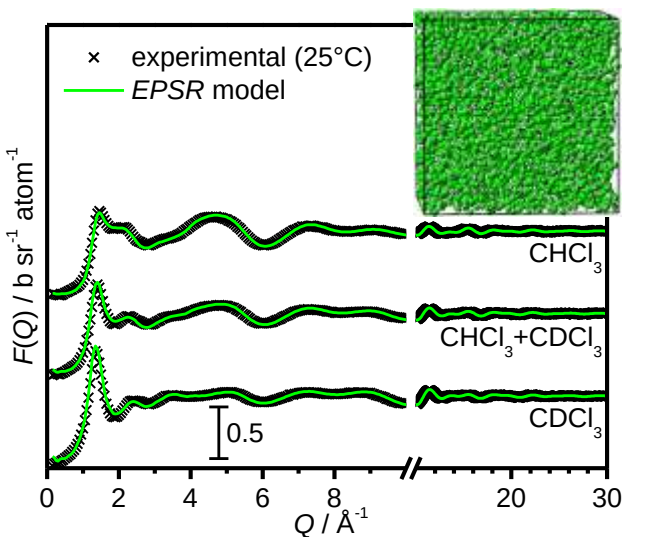

Figure 1. Experimental (black crosses) and calculated neutron diffraction data from an *EPSR*-derived model (solid green lines, inset structure).

The structural analysis of the *EPSR*-derived model shown in Figure 1 is carried out by calculating intermolecular pair-correlation functions such as $g_{C–H}(r, \theta, \phi)$ which gives the probability of the position of the H atom of a 2nd molecule with respect to the C atom of the reference molecule. For these analyses, the C atom of the reference molecule is positioned at the origin of the coordinate system, the H atom along the z_1 axis and one of the Cl atoms in the x_1z_1-plane as shown in Figure 2a. The position of the H atom of a 2nd molecule is then defined by a set of spherical coordinates including the radial C–H distance, r, as well as the polar and azimuthal angles θ and ϕ.

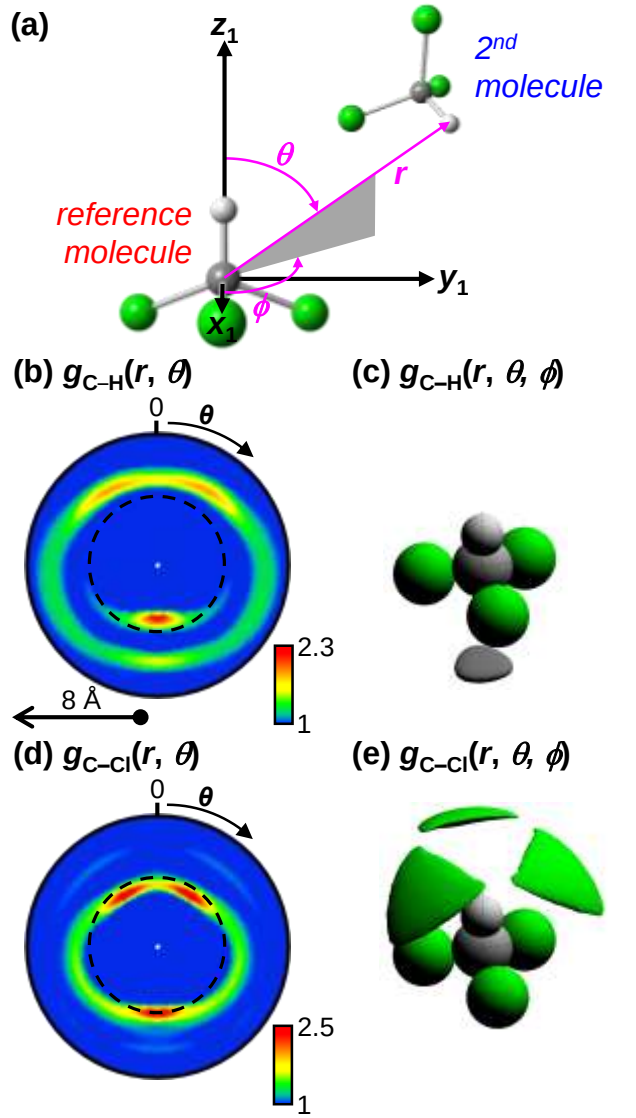

Figure 2. (a) Schematic illustration showing the fixed orientation of the reference molecule and the spherical coordinates that define the positions of atoms of a 2nd molecule in the coordination shell. (b, d) Contour plots of $g_{C–H}(r, \theta)$ and $g_{C–Cl}(r, \theta)$, respectively. The dashed circles indicate radial distances of 4.2 Å which were used as the upper limits for the spatial density functions in (c) $g_{C–H}(r, \phi, \theta)$ and (e) $g_{C–Cl}(r, \phi, \theta)$ both plotted with fractional isosurface levels of 0.1.

The most likely positions of H atoms in the coordination shell of $CHCl_3$ can be seen from the $g_{C–H}(r, \theta)$ function shown in Figure 2b. This function is averaged over ϕ, and depends therefore only on the radial C–H distance and θ. The most closely approaching H atoms are found at θ=180° (below the reference molecule) and at a C–H distance of 3.3 Å.

Three-dimensional structural information can be displayed using spatial density functions (SDFs) which make use of fractional isosurface levels. These highlight volumes where the pair-correlation function takes large values and contains specified fractions of the atoms.[12] The dashed circle in Figure 2b indicates the upper C–H distance limit used for the construction of the C–H SDF shown in Figure 2c. Again, it can be seen that the most likely position of H atoms is in $-z_1$ direction below the fully chlorinated face of the reference molecule.

The most likely locations of the closest Cl atoms on the other hand are found at C–Cl distances of 3.7 Å and θ values of about ±30° (Figure 2d). Slightly further away from the C centre there is also a high probability of finding Cl atoms at θ=180°. The three triangle-shaped lobes in the C–Cl SDF in Figure 2e also show that the most likely positions of Cl atoms are found above the reference molecule and that the Cl atoms of the 2nd molecule are preferentially in a staggered conformation with respect to the reference.

Detailed information on the relative orientations of the dipole moments of neighbouring molecules can be obtained from orientational correlation functions (OCFs).[13-16] Since molecules rotate about their centre of mass (COM), the origin of the coordinate system is now placed at the COM of the reference molecule and its dipole moment is aligned with the z_1 axis. The relative orientation of the dipole moment of a 2nd molecule with respect to the dipole moment of the reference is then defined by the angle α shown in Figure 3a. The contour plots in Figure 3a show the OCFs, $g_{COM–COM}(r, \alpha)$, for values of θ of 0, 45, 90, 135 and 180°.

A very strong tendency for stacking of molecules with collinear dipole alignment is indicated by large values of the OCFs at the positions labelled (1). The corresponding structure is labelled (1) in Figure 3b. At position (2), the OCF has values only slightly larger than one in the α range from 160 to 200°. This corresponds to an arrangement with anti-collinear dipole alignment in which the fully chlorinated faces of two molecules approach closely (structure (2) in Figure 3b). An anti-collinear dipole alignment, where two H atoms face each other (structure (3) in Figure 3(b)), is unlikely as indicated by the low value of the OCF at position (3). At θ angles of 45, 90 and 135° comparatively low degrees of orientational correlations are observed.

To determine the percentages of molecules that take part in stacks of $CHCl_3$ molecules with approximately collinear dipoles we define a C–H distance range from 2 to 4.2 Å and an H–C•••H angle range from θ=150 to 210° as the condition for polar stacking (*cf.* Figure 2b). As shown in Figure 4, 29.3 % of the molecules take part in polar stacks at 25°C and this number increases to 39.0 % at –53°C (10°C above the melting point). More than 1 % of the molecules take part in tetrameric stacks at 25°C and this percentage almost triples at –53°C. Considering that the average COM–COM distance in the stacks is ~4.2 Å (Figure 3a) the lengths of these constructs reach into the nanometre range.

It is interesting to note in this context that chloroform crystallises to a polar phase above 0.6 GPa with $P6_3$ space group symmetry.[17] This phase consists of stacked layers in which all dipole moments point in the direction of stacking. The ambient pressure phase is non-polar. However, it has been stated that the potential energy difference between parallel and antiparallel arrangements only very slightly favours antiparallel association in the ambient pressure phase.[17]

The orientational correlations of a wide range of liquids of small polar molecules have been reported including HF,[18] HCl,[19, 20] HBr,[15] HI,[14] H_2O,[21] H_2S,[22] CHF_3[23] and CH_3F.[23] Out of these, only HCl showed strong collinear dipole correlations.[19, 20] At a reduced temperature ($T_{red.}=T / T_{critical}$) of 0.59 the maximum value of $g_{COM–COM}(r, \alpha)$ was ~13 at θ=0°.[20] The corresponding value for $CHCl_3$ found here is 14.9 at a comparable $T_{red.}$ of 0.56 (Figure 3a). For CHF_3 and CH_3F,[23] weak orientational correlations have been found which are of a similar nature to those of CF_4.[24] For $CHBr_3$, no full OCF analysis has been carried out so far.[25]

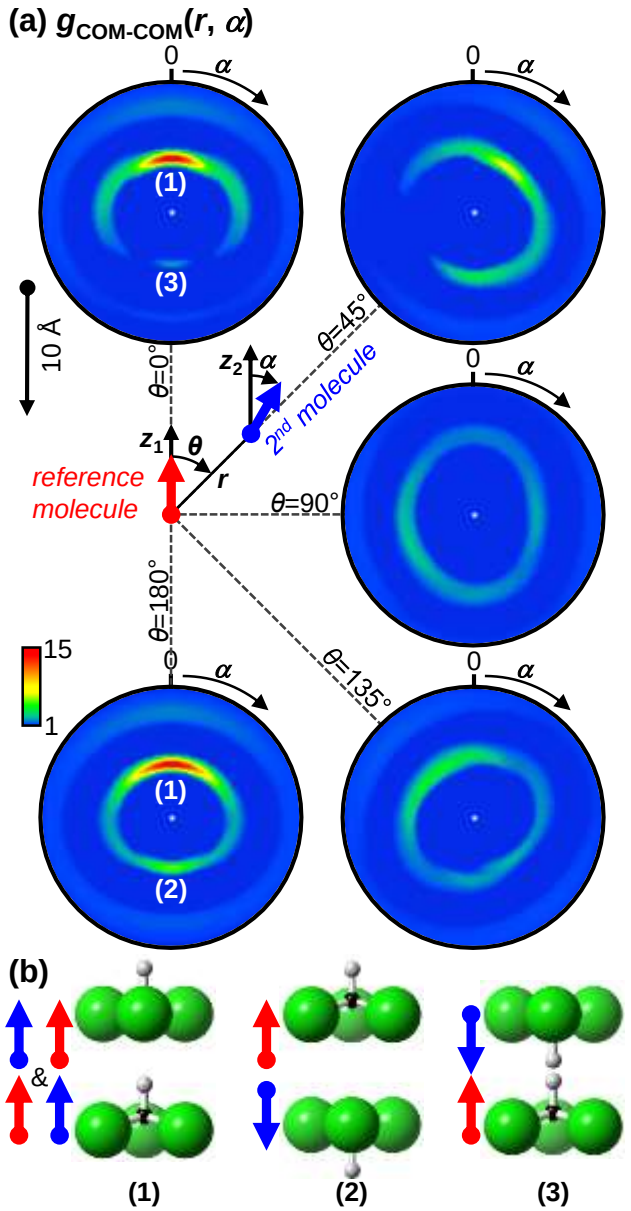

Figure 3. (a) Contour plots of $g_{COM-COM}(r, \alpha)$ for specified values of θ. The relative orientation of the dipole moment of a 2nd molecule is defined by the angle α and r is the centre of mass separation. The structures corresponding to positions (1-3) are shown in (b).

We note that there have been two earlier diffraction studies of $CHCl_3$.[26, 27] Early work by Bertagnolli *et al.*[26] suggested that the most favourable arrangement of two molecules in liquid chloroform is one in which the dipole axes are inclined with respect to each other at an angle of ~45° and the carbon atom of the second molecule is offset from the *z*-axis of the reference molecule (*cf.* structure 'A' in Fig. 8 in ref. 26). However, a later study of the same data, which used the Reverse Monte Carlo (*RMC*) approach for structure reconstruction, gave a quite different picture.[28] The set of radial pair-correlation functions derived in that work are similar to those from the present work (*cf.* Fig S2). However, in contrast to our work anti-parallel dipole alignments were found to dominate at low intermolecular distances in ref. 28.

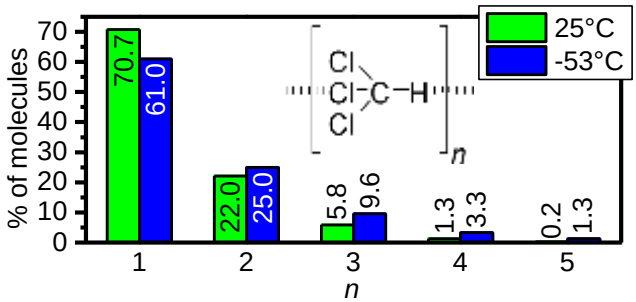

Figure 4. Length analysis of polar stacks of molecules using an H–C•••H angle range of 150-210° and an C–H distance range of 2.0-4.2 Å as the criterion for polar stacking.

More recently, Pothoczki *et al.* conducted a combined neutron / X-ray diffraction experiment which was also analysed with *RMC*.[27] The agreement of their radial pair-correlation functions with our functions shown in Fig. S2 is less clear due to the presence of sharp, and therefore unphysical, features in the former functions. These probably arise from the use of hard cut-offs within the *RMC* method to prevent atomic overlap. They also concluded that the strongest dipole-dipole correlations are anti-collinear with the fully chlorinated faces of two molecules approaching each other (*cf.* Fig. 10b in ref. 25).

As stated above, our results indicate a minor presence of anti-collinear arrangements. However, by far the most dominant structural features are collinear correlations. An important distinction between the previous *RMC* investigations[25-27] and the present study using *EPSR* is that the reference potentials used in the *EPSR* approach include Coulomb charges on the atoms (*cf.* Table S1) allowing the possibility of electrostatic ordering in a fashion which is consistent with the diffraction data. Such electrostatic ordering cannot be maintained within current *RMC* schemes. To underpin that our neutron-diffraction derived structural model using the *EPSR* approach is the most reliable reported so far we show in the *ESI* that our structural model is also consistent with X-ray diffraction data. Furthermore, we also show in the *ESI* that our structural model is in agreement with results from dielectric spectroscopy which suggest that parallel alignments of the dipole moments dominate in liquid chloroform.[29]

Conclusions

Liquid $CHCl_3$ displays some of the most pronounced collinear dipole correlations reported so far for the liquids of small polar molecules. Considerable percentages of the molecules are part of polar stacks at 25°C and even more at –53°C. Due to the collinear alignment of the dipole moments, the stacks have net dipole moments greater than those of individual $CHCl_3$ molecules. The lengths of these polar stacks reach the nanometre range and are therefore comparable in their dimension with a wide range of organic molecules. We propose that these 'super-dipole' aggregates are capable of strongly polarizing the electron clouds of nearby solutes thereby providing a favourable enthalpic contribution to dissolution and extraction processes. Overall, this effect could explain some of the outstanding properties of $CHCl_3$ as a solvent and it may potentially highlight a route to designing new high-performance solvents.

Notes and references

[a] Department of Chemistry, University College London, 20 Gordon Street, WC1H 0AJ London, UK, E-mail: c.salzmann@ucl.ac.uk

[b] Department of Chemistry, Durham University, South Road, Durham DH1 3LE, UK

[c] ISIS Facility, STFC Rutherford Appleton Laboratory, Harwell Oxford, Didcot OX11 0QX, UK

Electronic Supplementary Information (ESI) available: Materials, Neutron diffraction experiments, Data modelling, Structural analysis, Comparison with X-ray diffraction data. See DOI: 10.1039/c000000x/

1. A. R. Katritzky, D. C. Fara, H. Yang and K. Tämm, *Chem. Rev.*, 2004, **104**, 175-198.
2. C. Reichardt, *Org. Process Res. Dev.*, 2007, **11**, 105-113.
3. D. T. Bowron, J. L. Finney and A. K. Soper, *J. Am. Chem. Soc.*, 2006, **128**, 5119-5126.
4. *Solvent Extraction and Liquid Membranes: Fundamentals and Applications in New Materials*, CRC Press, 2008.
5. A. Puckner, *J. Am. Chem. Soc.*, 1901, **23**, 470-473.
6. M. J. Solomon and F. A. Crane, *J. Pharm. Sci.*, 1970, **59**.
7. P. Crews, J. Rodriguez and M. Jaspars, *Organic Structure Analysis*, Oxford University Press, New York, 1998.
8. A. K. Soper, *Chem. Phys.*, 1996, **202**, 295-306.
9. A. K. Soper, *Phys. Rev. B*, 2005, **72**, 104204.
10. A. K. Soper, *Chem. Phys.*, 2000, **258**, 121-137.
11. D. T. Bowron, J. L. Finney and A. K. Soper, *J. Chem. Phys.*, 2001, **114**, 6203-6219.
12. I. M. Svishchev and P. G. Kusalik, *J. Chem. Phys.*, 1993, **99**, 3049-3058.
13. C. G. Gray and K. E. Gubbins, *Theory of Molecular Fluids, Volume 1: Fundamentals*, Clarendon Press, Oxford, 1984.
14. A. K. Soper, C. Andreani and M. Nardone, *Phys. Rev. E*, 1993, **47**, 2598-2605.
15. C. Andreani, F. Menzinger, M. A. Ricci, A. K. Soper and J. Dreyer, *Phys. Rev. B*, 1994, **49**, 3811-3820.
16. A. K. Soper, *J. Chem. Phys.*, 1994, **101**, 6889-6901.
17. K. F. Dziubek and A. Katrusiak, *J. Phys. Chem. B.*, 2008, **112**, 12001-12009.
18. S. E. McLain, C. J. Benmore, J. E. Siewenie, J. Urquidi and J. F. C. Turner, *J. Am. Chem. Soc.*, 2004, **43**, 1952-1955.
19. C. Andreani, M. A. Ricci, M. Nardone, M. A. Ricci and A. K. Soper, *J. Chem. Phys.*, 1997, **107**, 214-221.
20. C. Andreani, *J. Mol. Liq.*, 1998, **78**, 217-223.
21. A. K. Soper, *J. Chem. Phys.*, 1994, **101**, 6888-6901.
22. G. Santoli, F. Bruni, M. A. Ricci and A. K. Soper, *Mol. Phys.*, 1999, **97**, 777-786.
23. J. Neuefeind, H. E. Fischer and W. Schröer, *J. Phys.: Condens. Matter*, 2000, **12**, 8765-8776.
24. I. Waldner, A. Bassen, H. Bertagnolli, K. Tödheide, G. Strauss and A. K. Soper, *J. Chem. Phys.*, 1997, **107**, 10667-10674.
25. S. Pothoczki, L. Temleitner and L. Pusztai, *J. Chem. Phys.*, 2011, **134**.
26. H. Bertagnoli and P. Chieux, *Mol. Phys.*, 1984, **51**, 617-631.
27. S. Pothoczki, L. Temleitner, S. Kohara, P. Jovari and L. Pusztai, *J. Phys. Condens. Matter*, 2010, **22**.
28. H. Bertagnolli, K. Goller and H. Zweier, *Ber. Bunsenges. Phys. Chem.*, 1995, **99**, 1168-1178.
29. P. H. Fries, *Mol. Phys.*, 1997, **90**, 841-853.

